Structural Engineering and Mechanics, Vol. 9, No. 3 (2000) 215-226
DOI: http://dx.doi.org/10.12989/sem.2000.9.3.215

Application of return mapping technique to multiple hardening concrete model

S.S. Eddie Lam†

Department of Civil and Structural Engineering, The Hong Kong Polytechnic University, Hung Hom, Hong Kong

Bo Diao‡

Department of Civil Engineering, Northern Jiaotong University, Beijing, China

Abstract. Computational procedure within the framework of return mapping technique has been presented to integrate the constitutive behavior of a concrete model. Developed by Ohtani and Chen, this concrete model is based on multiple hardening concept, and is rate-independent and associative. Consistent tangent operator suitable for finite element analysis is derived to preserve the rate of convergence. Accuracy of the integration technique is verified and compared with available experimental data. Computational efficiency is demonstrated by comparing with results based on elasto-plastic tangent.

Key words: concrete; multiple hardening; plasticity; return mapping; consistent tangent operation.

1. Introduction

Accurate prediction of the inelastic behavior of concrete depends to a large extent on the constitutive model and the algorithm used in the analysis. In recent years, considerable research has been focused on the mechanical behavior of concrete and in the development of appropriate constitutive models. Among others, rate-independent concrete models were developed by Chen and Chen (1975), Willam and Warnke (1975), Han and Chen (1985), and Pietruszczak *et al.* (1988), Bazant and Kim (1979), and Dragon and Mroz (1979) applied the plastic-fracture theory; whilst damage theory was used by Gilles *et al*. (1995). However, aspects on the numerical treatment of concrete models are not developed at an equal pace. The main thrust of this study is to implement a computational procedure to integrate the constitutive behavior of a concrete model based on multiple hardening. Application of multiple hardening to concrete was first proposed by Murray *et al.* (1979) and was generalized by Ohtani and Chen (1988). The concrete model assumes rate-independent plasticity and associated flow rule. Performance of this concrete model for practical problems was reported by Chen (1994) and has been demonstrated to be of acceptable accuracy.

In the analysis of inelastic problems by the finite element method, solution at global level is achieved through consecutive load increments. In each load step, equilibrium equations are solved

† Assistant Professor
‡ Associate Professor

iteratively, for instance, by the Newton-Raphson procedure. For rate-independent plasticity problems, the return mapping technique has been demonstrated to be highly efficient. Application of the technique was first reported by Krieg and Krieg (1977) and by Schreyer *et al.* (1979). Their work has stimulated a spate of publications (Simo and Taylor 1985, Simo and Hughes 1987, Matthies 1989, Hofestter *et al.* 1993, Hofstetter and Mang 1994, Matzenmiller and Taylor 1994). Among others, Simo *et al.* (1988), Ghosh and Kikuchi (1988), Simo and Govindjee (1991), and Meschke (1996) applied the technique to visco-plasticity problems; Schellekens and Borst (1990) developed return mapping algorithms for anisotropic plasticity; and Hofstetter and Taylor (1990) considered non-associative plasticity. In this study, the return mapping technique is extended to embrace the analysis of concrete material.

In what follows, the general development of the approach is presented. Applications involving bi-axial stress states have been described. The results are compared with experimental data obtained by Kupfer *et al*. (1969) and Tasuji *et al.* (1978). Efficiency of the technique is further demonstrated by comparison with the results based on elasto-plastic tangents (Hinton and Owen 1980).

2. Governing equations of Ohtani-Chen model

Geometry of the yield surface assumed by Ohtani and Chen (1988) is having the same shape as the Chen and Chen (1975) model. The yield surface is represented mathematically by a yield function f with N multiple hardening parameters q_1, q_2,..., q_N.

$$f(\{\sigma\}, q_1, q_2, \ldots, q_N)=0 \tag{1}$$

where $\{\sigma\}$ is the stress vector, and q_M is the Mth hardening parameter. The latter is an unique function of the Mth damage parameter μ_M, or

$$q_M=q_M(\mu_M) \tag{2}$$

μ_M is related to α_M, a scalar representing the effect of damage to the Mth hardening mode.

$$\mu_M=\int d\mu_M=\int \alpha_M d\varepsilon_p \tag{3}$$

Details in the determination of the coefficient α_M is described by Ohtani and Chen (1988). The equivalent plastic strain ε_p is the cumulation of the increment of equivalent plastic strain $d\varepsilon_p$.

$$\varepsilon_p=\int d\varepsilon_p \tag{4}$$

The stress-strain relationship is assumed to obey the Hooke's Law,

$$\{\sigma\}=\{D\}(\{\varepsilon\}-\{\varepsilon^p\}) \tag{5}$$

where $\{\varepsilon^p\}$ is the plastic strain vector, $\{\varepsilon\}$ is the total strain vector and $\{D\}$ is the elastic constitutive matrix for isotropic material. The plastic strain increment induced during plastic loading is obtained by enforcing the associated flow rule, i.e.

$$\{d\varepsilon^p\}=\lambda\left\{\frac{\partial f}{\partial\sigma}\right\} \tag{6}$$

where λ is the proportional factor, and a positive scalar.

Consistent with the displacement-type finite element approach, it is assumed that the state variables $\{\sigma\}$, $\{\varepsilon^p\}, \lambda$ and q_i are computed from a given deformation history or $\{\varepsilon\}$. New values of the state variables are obtained by integration of the constitutive equations projected from an initial state. In this study, the return mapping technique is used in the integration in the manner now described.

3. Integration scheme

Earlier treatments on plasticity problems for concrete employ a direct method to integrate the state variables. Substitution of Eqs. (5) and (6) into the consistency equation

$$df=\left\{\frac{\partial f}{\partial \sigma}\right\}^T\{d\sigma\}+\frac{\partial f}{\partial q_j}\frac{\partial q_j}{\partial \varepsilon_p}d\varepsilon_p=0 \tag{7}$$

the plasticity problem is reduced to the computation of a single unknown λ.

$$\lambda=\frac{\left\{\frac{\partial f}{\partial \sigma}\right\}^T\{D\}\{\delta\varepsilon\}}{\left\{\frac{\partial f}{\partial \sigma}\right\}^T\{D\}\left\{\frac{\partial f}{\partial \sigma}\right\}-\left(\frac{\partial f}{\partial q_j}\frac{\partial q_j}{\partial \varepsilon_p}\right)\sqrt{\left\{\frac{\partial f}{\partial \sigma}\right\}^T\left\{\frac{\partial f}{\partial \sigma}\right\}}} \tag{8}$$

where $\{\delta\varepsilon\}$ is the change in total strain. Substituting λ into Eq. (6) gives the plastic strain increment. By considering the governing equations in incremental form, the other state variables are computed. In general, the updated state variables will not satisfy the yield condition. As a result, there are possible errors associated with the yield function and the flow rule. The latter is due to inaccurate prediction of the plastic strain increment. To eliminate these errors, an iterative scheme local to a set of state variables is implemented.

Let $\{\sigma^{(k)}\}$, $\{\varepsilon^{p,(k)}\}$, $q_i^{(k)}$ and $\lambda^{(k)}$ be an approximate solution with respect to a new deformation $\{\varepsilon\}$. Here the superscript (k) represents the values at an iterative step k in the computation of the state variables. Errors associated with the approximate solution are

$$r_f^{(k)}=f^{(k)}(\{\sigma^{(k)}\}, q_1^{(k)}, q_2^{(k)}, \ldots, q_N^{(k)}) \tag{9}$$

$$\{r_\varepsilon^{(k)}\}=\{\varepsilon^{p,(k)}\}-\{\varepsilon^p\}-\lambda^{(k)}\left\{\frac{\partial f^{(k)}}{\partial \sigma}\right\} \tag{10}$$

where $r_f^{(k)}$ and $\{r_\varepsilon^{(k)}\}$ are the residuals for the yield function and plastic loading respectively. $\{\varepsilon^p\}$ is the plastic strain at the beginning of the iterative process. Improved solution for the next iteration denoted by superscript $(k+1)$ is obtained by equating to zero the curtailed Taylor's expansion of the residuals in the neighborhood of the approximate solution at iteration (k). Thus,

$$r_f^{(k)}+\left\{\frac{\partial f^{(k)}}{\partial \sigma}\right\}^T\{\Delta\sigma^{(k+1)}\}+\frac{\partial f^{(k)}}{\partial q_j}\frac{\partial q_j^{(k)}}{\partial \varepsilon_p}\Delta\varepsilon_p^{(k+1)}=0 \tag{11a}$$

$$\{r_\varepsilon^{(k)}\}-\{\Delta\varepsilon^{p,(k+1)}\}+\Delta\lambda^{(k+1)}\left\{\frac{\partial f^{(k)}}{\partial \sigma}\right\}+\lambda^{(k)}\left(\left\{\frac{\partial^2 f^{(k)}}{\partial \sigma^2}\right\}\{\Delta\sigma^{(k+1)}\}+\left\{\frac{\partial^2 f^{(k)}}{\partial \sigma \partial q_j}\right\}\frac{\partial q_j^{(k)}}{\partial \varepsilon_p}\Delta\varepsilon_p^{(k+1)}\right)=0 \tag{11b}$$

where,

$$\frac{\partial f^{(k)}}{\partial q_i}\frac{\partial q_i^{(k)}}{\partial \varepsilon_p}=\sum_{j=1}^{N}\frac{\partial f^{(k)}}{\partial q_j}H_j^p\alpha_j \tag{12a}$$

$$\left\{\frac{\partial^2 f^{(k)}}{\partial\sigma\partial q_j}\right\}\frac{\partial q_j^{(k)}}{\partial \varepsilon_p}=\sum_{j=1}^{N}\left\{\frac{\partial^2 f^{(k)}}{\partial\sigma\partial q_j}\right\}H_j^p\alpha_j \tag{12b}$$

$$H_j^p=\frac{\partial q_j^{(k)}}{\partial \mu_j} \tag{12c}$$

$\{\Delta\sigma^{(k+1)}\}$, $\{\Delta\varepsilon^{p,(k+1)}\}$ and $\Delta\lambda^{(k+1)}$ are incremental quantities associated with the iterative step. Improved values of $\{\varepsilon^{p,(k+1)}\}$and $\lambda^{(k+1)}$ are obtained by summation over the number of iterative steps, i.e.,

$$\{\varepsilon^{p,(k+1)}\}=\{\varepsilon^p\}+\sum_{j=1}^{k+1}\{\Delta\varepsilon^{p,(j)}\} \tag{13a}$$

$$\lambda^{(k+1)}=\sum_{j=1}^{k+1}\Delta\lambda^{(j)} \tag{13b}$$

$\{\sigma^{(k+1)}\}$ is computed through the stress-strain relationship.

$$\{\sigma^{(k+1)}\}=\{\sigma\}+\{D\}(\{\delta\varepsilon\}-\{\varepsilon^{p,(k+1)}\}+\{\varepsilon^p\}) \tag{13c}$$

where $\{\sigma\}$, $\{\varepsilon^p\}$and q_i be a set of variables representing an initial state that satisfies Eqs. (1) to (6). Linearizing the equivalent plastic strain increment $\Delta\varepsilon_p^{(k+1)}$ and plastic strain increment $\{\Delta\varepsilon^{p,(k+1)}\}$ by

$$\Delta\varepsilon_p^{(k+1)}=\Delta\lambda^{(k+1)}\sqrt{\left\{\frac{\partial f^{(k)}}{\partial\sigma}\right\}^T\left\{\frac{\partial f^{(k)}}{\partial\sigma}\right\}} \tag{14a}$$

$$\{\Delta\varepsilon^{p,(k+1)}\}=-\{D\}^{-1}\{\Delta\sigma^{(k+1)}\} \tag{14b}$$

and substituting into Eqs. (11a) and (11b), the problem is reduced to the computation of a single unknown $\Delta\lambda^{(k+1)}$.

$$\Delta\lambda^{(k+1)}=\frac{r_f^{(k)}-\left\{\frac{\partial f^{(k)}}{\partial\sigma}\right\}^T\{\chi\}\{r_\varepsilon^{(k)}\}}{\psi+\left\{\frac{\partial f^{(k)}}{\partial\sigma}\right\}^T\{\chi\}\left\{\frac{\partial f^{(k)}}{\partial\sigma}\right\}} \tag{15}$$

where $\{\chi\}$ is a square matrix expressed as

$$\{\chi\}=\left[\{D\}^{-1}+\lambda^{(k)}\left\{\frac{\partial^2 f^{(k)}}{\partial\sigma^2}\right\}\right]^{-1} \tag{16a}$$

and ψ is a scalar in the form of

$$\psi=\lambda^{(k)}\left\{\frac{\partial f^{(k)}}{\partial\sigma}\right\}^T\{\chi\}\left(\sum_{j=1}^{N}\left\{\frac{\partial^2 f^{(k)}}{\partial\sigma\partial q_j}\right\}H_j^p\alpha_j\right)\sqrt{\left\{\frac{\partial f^{(k)}}{\partial\sigma}\right\}^T\left\{\frac{\partial f^{(k)}}{\partial\sigma}\right\}}-\left(\sum_{j=1}^{N}\frac{\partial f^{(k)}}{\partial q_j}H_j^p\alpha_j\right)\sqrt{\left\{\frac{\partial f^{(k)}}{\partial\sigma}\right\}^T\left\{\frac{\partial f^{(k)}}{\partial\sigma}\right\}} \tag{16b}$$

Similar expressions are also obtained by Hofstetter and Mang (1994). Their study has incorporated additional internal variables, which are not presented in this concrete model.

Increment of the effective plastic strain is obtained by

$$\Delta\varepsilon_p^{(k+1)}=\sqrt{\{\Delta\varepsilon^{p,(k+1)}\}\{\Delta\varepsilon^{p,(k+1)}\}} \tag{17}$$

and the hardening parameters $q_j^{(k+1)}$ are obtained through the following relations

$$q_j^{(k+1)}=q_j+\sum_{i=1}^{k+1}\Delta q_i^{(j)} \tag{18a}$$

$$\Delta q_j^{(k+1)}=H_j^p\alpha_j\Delta\varepsilon_p^{(k+1)} \tag{18b}$$

4. Consistent tangent operator

In every load step, the Newton-Raphson procedure is applied at global level to enforce the equilibrium condition. Linearization of the nonlinear problem is achieved by the tangent operator, which is defined as

$$\{d\sigma\}=\{C\}\{d\varepsilon\} \tag{19}$$

To ensure an optimal rate of convergence, the tangent operator is obtained in a manner consistent with the integration algorithm (Simo and Taylor 1985). Computation of the tangent operator is achieved based on the state variables obtained at the end of iteration. For simplicity, the superscript (k+1) is omitted in the equations that follow. Considering the constitutive relation, flow rule and the yield condition in incremental form

$$\{d\sigma\}=\{D\}(\{d\varepsilon\}-\{d\varepsilon^p\}) \tag{20a}$$

$$\{d\varepsilon^p\}=d\lambda\left\{\frac{\partial f}{\partial\sigma}\right\}+\lambda\left(\left\{\frac{\partial^2 f}{\partial\sigma^2}\right\}\{d\sigma\}+\left\{\frac{\partial^2 f}{\partial\sigma\partial q_j}\right\}\frac{\partial q_j}{\partial\varepsilon_p}d\varepsilon_p\right) \tag{20b}$$

$$df=\left\{\frac{\partial f}{\partial\sigma}\right\}^T\{d\sigma\}+\frac{\partial f}{\partial q_j}\frac{\partial q_j}{\partial\varepsilon_p}d\varepsilon_p=0 \tag{20c}$$

Futher manipulation, the tangent operator is obtained.

$$\{C\}=\{\chi\}-\frac{1}{h}\{\chi\}\left\{\frac{\partial f}{\partial\sigma}\right\}\left\{\frac{\partial f}{\partial\sigma}\right\}^T\{\chi\}-\frac{1}{h}\lambda\{\chi\}\left\{\frac{\partial^2 f}{\partial\sigma\partial q_j}\right\}\frac{\partial q_j}{\partial\varepsilon_p}\left\{\frac{\partial f}{\partial\sigma}\right\}^T\{\chi\}\sqrt{\left\{\frac{\partial f}{\partial\sigma}\right\}^T\left\{\frac{\partial f}{\partial\sigma}\right\}} \tag{21}$$

where h is a scalar defined as

$$h=\left\{\frac{\partial f}{\partial\sigma}\right\}^T\{\chi\}\left\{\frac{\partial f}{\partial\sigma}\right\}-\left(\sum_{j=1}^{N}\frac{\partial f}{\partial q_j}H_j^p\alpha_j\right)\sqrt{\left\{\frac{\partial f}{\partial\sigma}\right\}^T\left\{\frac{\partial f}{\partial\sigma}\right\}}$$

$$+\lambda\left\{\frac{\partial f}{\partial \sigma}\right\}^T\{\chi\}\left(\sum_{j=1}^{N}\left\{\frac{\partial^2 f}{\partial\sigma\partial q_j}\right\}H_j^p\alpha_j\right)\Bigg/\sqrt{\left\{\frac{\partial f}{\partial \sigma}\right\}^T\left\{\frac{\partial f}{\partial \sigma}\right\}} \tag{22}$$

5. Application

Accuracy and efficiency of the aforementioned procedure is demonstrated through applications on the Chen and Chen (1975) concrete model. Yield surface is described by a quadratic function with three independent variables determined from three separate tests, namely uniaxial tension, uniaxial compression and biaxial compression. The yield function or loading surface is represented by

$$f(\{\sigma\},\ \sigma_c,\ \sigma_{bc},\ \sigma_t)=0 \tag{23}$$

where σ_c, σ_{bc} and σ_t are the hardening parameters representing the yield stresses in uniaxial compression, biaxial compression and uniaxial tension respectively.

The loading surface in the compression-compression region is

$$f(\{\sigma\},\ \sigma_c,\ \sigma_{bc},\ \sigma_t)=J_2+\frac{1}{3}A_cI_1-\tau_c^2=0 \tag{24a}$$

$$A_c=\frac{\sigma_{bc}^2-\sigma_c^2}{2\sigma_{bc}-\sigma_c} \tag{24b}$$

$$\tau_c^2=\frac{\sigma_c\sigma_{bc}(2\sigma_c-\sigma_{bc})}{3(2\sigma_{bc}-\sigma_c)} \tag{24c}$$

The loading surface in the tension-tension or tension-compression region is

$$f(\{\sigma\},\ \sigma_c,\ \sigma_{bc},\ \sigma_t)=J_2-\frac{1}{6}I_1^2+\frac{1}{3}A_tI_1-\tau_t^2=0 \tag{25a}$$

$$A_t=\frac{\sigma_c-\sigma_1}{2} \tag{25b}$$

$$\tau_t^2=\frac{\sigma_c\sigma_1}{6} \tag{25c}$$

where J_2 and I_1 are the second invariant of deviatoric stress and the first invariant of stress respectively. The first and second derivatives of the yield surface are included in the Appendix.

The present computational procedure is implemented to predict the constitutive behavior of concrete. Strain increments are controlled by the arc-length method (Crisfield 1991). The results are compared with experimental data reported by Kupfer *et al.* (1969) and Tasuji *et al.* (1978). Stress conditions include both uniaxial and biaxial stress states.

The following notations are introduced. f_{bc}, f_c and f_t represent the initial yield stresses at equal biaxial compression, uniaxial compression and uniaxial tension respectively, whereas f_{bc}', f_c' and f_t' are the respective counterparts at ultimate condition.

5.1. Comparison with Kupfer's data

Stress-strain relationships for concrete when subjected to biaxial stress were obtained experimentally by Kupfer *et al*. (1969). Predictions and comparisons with the experimental results have been conducted earlier by Ohtani and Chen (1988). Material properties for concrete are the same as those used in the previous study with f_{bc}'/f_c'=1.15, f_t'/f_c'=0.091, f_c/f_c'=0.60, f_{bc}/f_{bc}'=0.45, f_t/f_t'=0.50, E/f_c'=990 and ν=0.20.

Figs. 1(a) to (i) shows the stress-strain relationships for different stress ratios (σ_1:σ_2:σ_3). Figs. 2(a) to (c) gives the variation of volumetric strain against stress. All stresses and strains are assumed to be positive for tension and negative for compression. Not presented in the figures are the results obtained by Ohtani and Chen (1988), as they are in close agreement with the results obtained by the present study over the whole loading range. The results agree well with the experimental data, especially in the compression-compression loading cases. Similar discrepancies have also been observed by Ohtani and Chen (1988) in their prediction of the negative strains in tension-tension and tension-compression loading cases.

5.2. Comparison with Tasuji's data

Similar experimental studies were conducted by Tasuji *et al.* (1978). Comparison with the experimental data was preformed by Ohtani and Chen (1988) and is also repeated in this study. Material properties for concrete are f_{bc}'/f_c'=1.04, f_t'/f_c'=0.09, f_c/f_c'=0.60, f_{bc}/f_{bc}'=0.45, f_t/f_t'=0.50, E/f_c'=600 and ν = 0.22.

Results from the present study agree well with those obtained previously by Ohtani and Chen (1988). Fig. 3 shows the stress-strain relationships at different stress ratios. The discrepancies in the trends of the nonlinear response are similar to what has been observed in the comparison with Kupfer's data. This further demonstrates that the difference is inherited in the concrete model and is not due to the computational procedure.

5.3. Efficiency of return mapping technique

Efficiency of the present formulation is examined by comparing with an approach based on a forward Euler method and elasto-plastic tangent. Increments of the state variables are obtained by applying Eq. (8) in the manner as described earlier. The elasto-plastic tangent is obtained by enforcing the consistency condition by applying Eqs. (6), (8) and (20a),

$$\{C\}=\{D\}-\frac{\{D\}\left\{\frac{\partial f}{\partial\sigma}\right\}\left\{\frac{\partial f}{\partial\sigma}\right\}^T\{D\}}{\left\{\frac{\partial f}{\partial\sigma}\right\}^T D\left\{\frac{\partial f}{\partial\sigma}\right\}-\left(\sum_{m=1}^{N}\frac{\partial f}{\partial q_m}H_m\alpha_m\right)\sqrt{\left\{\frac{\partial f}{\partial\sigma}\right\}^T\left\{\frac{\partial f}{\partial\sigma}\right\}}} \tag{26}$$

with the approximation that $\{d\varepsilon\}=\{\delta\varepsilon\}$.

Again making use of Kupfer's (1969) experimental data, predictions by the present approach and the elasto-plastic tangent are included in Figs. 4 and 5, giving the trend of convergence with increasing number of increments. Two different stress ratios have been considered, namely (σ_1:σ_2:σ_3)=(−1.0, −1.0, 0.0) and (σ_1:σ_2:σ_3)=(−1.0, 0.103, 0.0) respectively. In these applications, although the

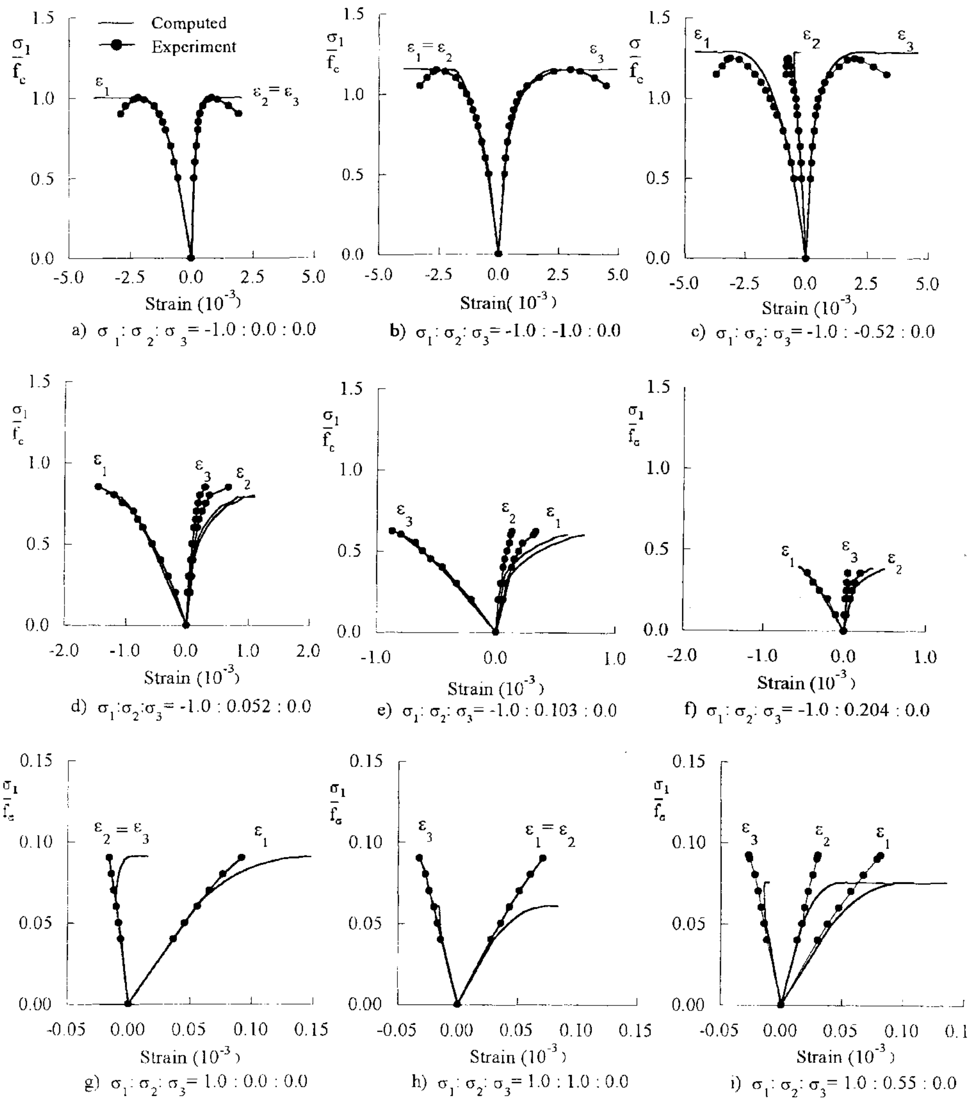

Fig. 1 Comparison of computed and experimental data (by Kupfer *et al.*): Stress-strain relationship

convergence exhibited by both approaches appears to be satisfactory, the present approach yields faster rate of convergence. Reasonable results are obtained in the two cases using 15 and 25 increments respectively, which are in close agreement with those obtained using 200 increments. The use of elasto-plastic tangent requires 200 and 400 increments respectively to achieve solutions with similar accuracy for these two cases. In the computation with 15 increments case in Fig. 4, analysis based on elasto-plastic tangent experiences convergence difficulties when the stress approaches 84% of the ultimate stress. This further demonstrates that analysis based on the use of elasto-plastic tangent has to be conducted at small increments, otherwise the projected state variables will not correspond well with the yield surface. Such difficulties are not encountered in the present approach, and relatively large increments can be allowed in the analysis with minimum effect on the accuracy of the solution.

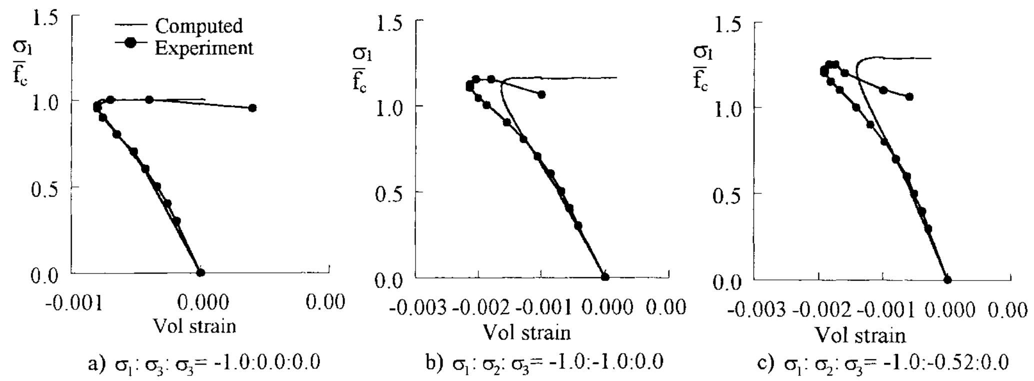

Fig. 2 Comparison of computed and experimental (by Kupfer *et al.*): Stress versus volumetric strain

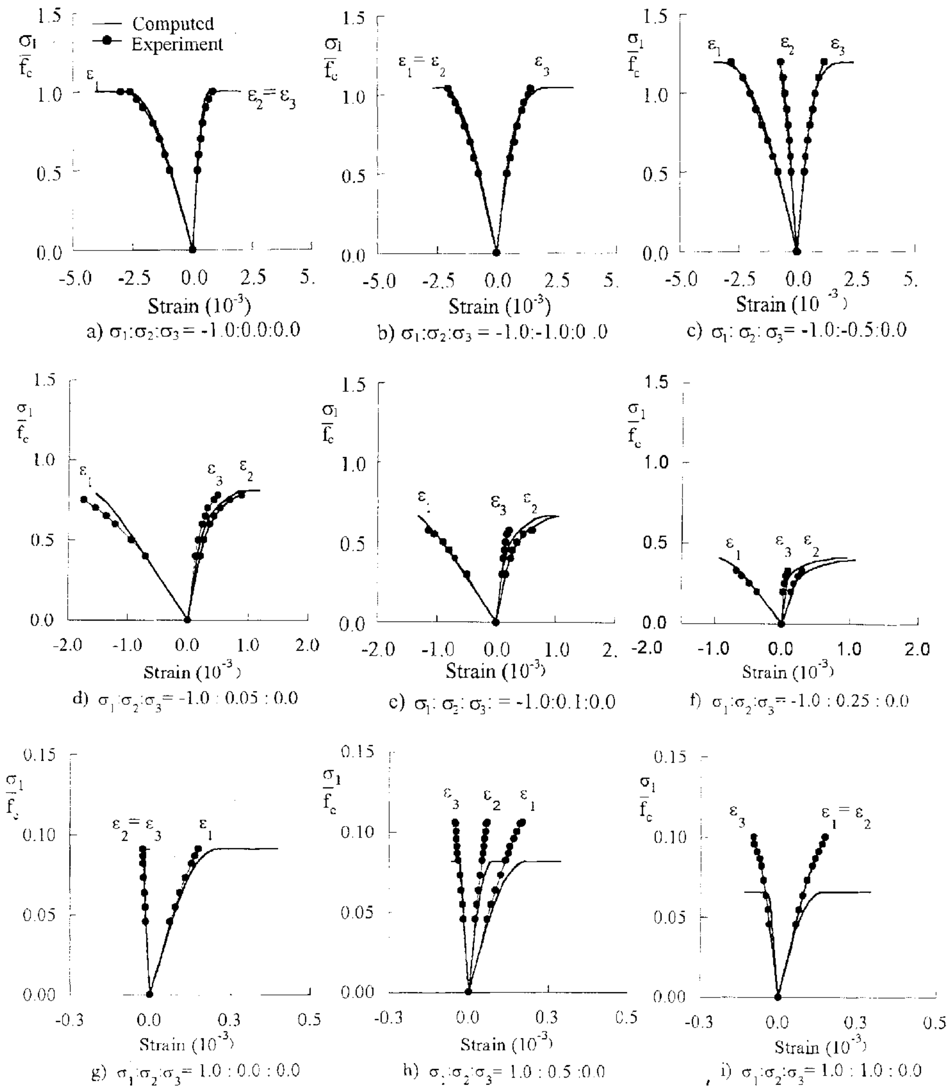

Fig. 3 Comparison of computed and experimental data (by Tasuji *et al.*): Stress-strain relationship

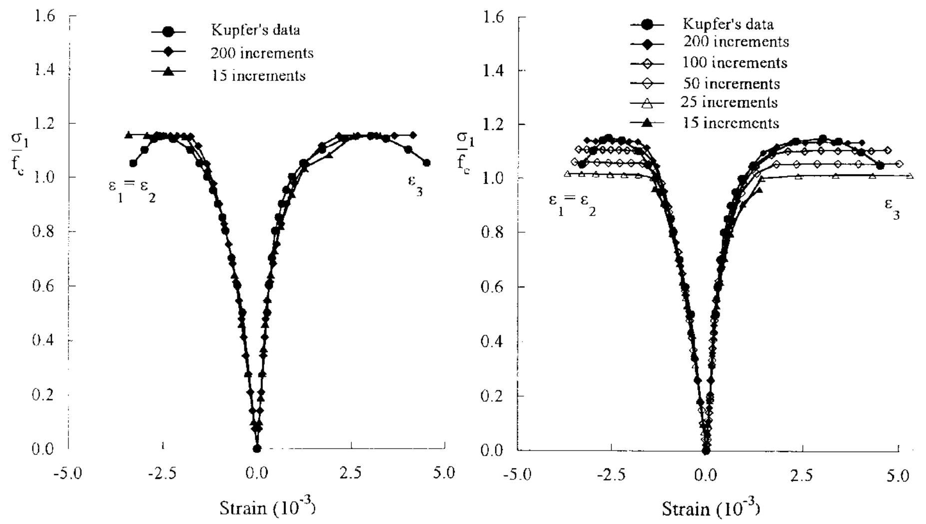

a) Present study b) Elasto-plastic tangent

Fig. 4 Convergence of stress-strain relationship with number of increments: $\sigma1$:$\sigma2$:$\sigma3$ = –1.0:–1.0:0.0

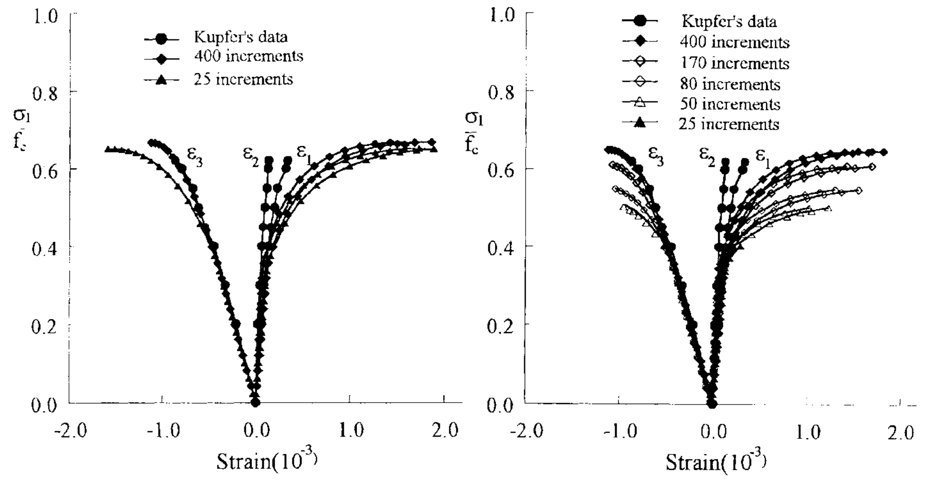

a) Present study b) Elesto-plastic tangent

Fig. 5. Convergence of stress-strain relationship with number of increments: $\sigma1$:$\sigma2$:$\sigma3$ = –1.0:0.103:0.0

6. Conclusions

Computation procedure based on the return mapping technique has been presented to integrate the constitutive behavior of a concrete model based on multiple hardening concept. The concrete model was developed previously by Ohtani and Chen, and assumes to be rate-independent and associative. The consistent tangent operator suitable for the finite element analysis has been derived.

Efficiency and accuracy of this present approach are tested against two sets of experimental data presented by Kupfer *et al.* (1969) and Tasuji *et al.* (1978). The predictions agree well with the experimental data and previous studies. This has served to verify the technique. Further comparisons are made with the results obtained based on the elasto-plastic tangent. It has been demonstrated that the present technique has the advantage of computational economy.

Acknowledgements

The authors are grateful for the financial support provided by the Department of Civil and Structural Engineering, The Hong Kong Polytechnic University.

References

Bazant, Z.P. and Kim, S. (1979), "Plastic-fracturing theory for concrete", *J. Engng. Mech., ASCE*, **105**(3), 407-428.

Chen, A.C.T. and Chen, W.F. (1975), "Constitutive relations for concrete", *J. Engng. Mech., ASCE*, **101**(4), August, 465-479.

Chen, W.F. (1994), "Theory of concrete plasticity", "Implementation and application for concretes", *Constitutive Equations for Engineering Materials, II: Plasticity and Modeling*, Elsevier.

Crisfield, M.A. (1991), *Non-linear Finite Element Analysis of Solids and Structures*, John Wiley & Sons.

Dragon, A. and Mroz, Z. (1979), "A continuum model for plastic-brittle behavior of rock and concrete", *Int. J. Engng. Sci.*, **17**.

Ghosh, S. and Kikuchi, N. (1988), "Finite element formulation for the simulation of hot sheet metal forming processes", *Int. J. Engng. Sci.*, **26**(2), 143-161.

Gilles, P.C., Borderie, C.L. and Fichant, S. (1995), "Applications and comparisons with plasticity and fracture mechanics", *Damage Mechanics of Concrete Modeling*, 17-36.

Han, D.J. and Chen, W.F. (1985), "A nonuniform hardening plasticity model for concrete materials", *J. Engng. Mech., ASCE*, **4**(4), December, 283-302.

Hinton, E. and Owen, D.R.J. (1980), *Finite Elements in Plasticity: Theory and Practice*, Pineridge Press, Swansea, Wales.

Hofstetter, G. and Taylor, R.L. (1990), "Non-associative Drucker-Prager plasticity at finite strains", *Comm. in Appl. Num. Meth.*, **6**, 583-589.

Hofstetter, G., Simo J.C. and Taylor, R.L. (1993), "A modified cap model: Closest point solution algorithms", *Computers and Structures*, **46**(2), 203-214.

Hofstetter, G. and Mang, H.A. (1994), *Computational Mechanics of Reinforced Concrete Structures*, Printed in Germany.

Krieg, R.D. and Krieg, D.B. (1977), "Accuracies of numerical solution methods for the elastic-perfectly plastic model", *J. of Pres. Ves. Tech., Trans ASME*, Nov., 510-515.

Kupfer, H., Hilsdorf, H.K. and Rusch, H. (1969), "Behavior of concrete under biaxial stresses", *ACI Journal*, August, 656-665.

Matthies, H.G. (1989), "A decomposition method for the integration of the elastic-plastic rate problem", *Int. J. Numer. Meth. Engng.*, **28**, 1-11.

Matzenmiller, A. and Taylor, R.L. (1994), "A return mapping algorithm for isotropic elastoplasticity", *Int. J. Numer. Meth. Engng.*, **37**, 813-826.

Meschke, G. (1996), "Consideration of aging of shotcrete in the context of a 3-D viscoplastic material model", *Int. J. Numer. Meth. Engng.*, **39**, 3123-3143.

Murray, D.W., Chitnuyanondh, L., Rijub-Agha, K.Y. and Wong, C. (1979), "Concrete plasticity theory for biaxial stress analysis", *J. of Engng. Mech., ASCE*, **105**(6), December, 989-1006.

Ohtani, Y. and Chen, W.F. (1988), "Multiple hardening plasticity for concrete material", *J. of Engng. Mech., ASCE*, **114**(11), 1890-1910.

Pietruszczak, S., Jiang, J. and Mirza, F.A. (1988), "An elastoplastic constitutive model for concrete", *Int. J. Solids Struct.*, **24**(7), 705-722.

Schellekens, J.C.J. and Borst, R.D. (1990), "The use of the Hoffman yield criterion in finite element analysis of anisotropic composites", *Comp. & Struct*., **37**(6), 1097-1096.
Schreyer, H.L., Kulak, R.F. and Kramer, J.M. (1979), "Accurate numerical solutions for elastic-plastic models", *J. of Pres. Ves. Tech., Trans ASME*, August, 226-234.
Simo, J.C. and Taylor, R.L. (1985), "Consistent tangent operators for rate-independent elastoplasticity", *Comp. Meth. in Appl. Mech. and Engng*., **48**, 101-118.
Simo, J.C. and Hughes, T.J.R. (1987), "General return mapping algorithms for rate-independent plasticity", *Constitutive Laws for Material: Theory and Applications*, eds. C.S. Desai *et al*., Elsevier Sci Publishing Co Inc.
Simo, J.C., Kennedy, J.G. and Godvindjee, S. (1988), "Unconditionally stable return mapping algorithms for non-smooth multi-surface plasticity amenable to exact linearization", *Int. J. Numer. Meth. Engng*., **26**, 2161-2115.
Simo, J.C. and Govindjee, S. (1991), "Non-linear B-stability and symmetry preserving return mapping algorithms for plasticity and viscoplasticity", *Int. J. Numer. Meth. Engng.*, **31**, 151-176.
Tasuji, M.E., Slate, F.O. and Nilson, A.H. (1978), "Stress-strain response and fracture of concrete in biaxial loading", *ACI Journal, July*, 306-312.
Willam, K.J. and Warnke, E.P. (1975), "Constitutive model for the triaxial behaviour of concrete", Int. Asso. for Bridge and Struct. Engng., Seminar on concrete structure subjected to triaxial stresses, *IABSE Proceedings*, **19**, 1-30.

Appendix

First derivatives of the Chen-Chen loading surface are

$$\frac{\partial f}{\partial \sigma_{ij}}=\left(\frac{1}{3}A+nI_1\right)\delta_{ij}+s_{ij}$$

where A=A_c and n=0 in the compression-compression region, and A=A_t and n=–1/3 otherwise.
In the compression-compression region:

$$\frac{\partial f}{\partial \sigma_c}=(I_1+2\sigma_{bc})*\frac{\sigma_c^2-4\sigma_c\sigma_{bc}+\sigma_{bc}^2}{3.0(2\sigma_{bc}-\sigma_c)^2},\ \frac{\partial f}{\partial \sigma_{bc}}=(I_1+\sigma_c)*\frac{2(\sigma_c^2-\sigma_c\sigma_{bc}+\sigma_{bc}^2)}{3.0(2\sigma_{bc}-\sigma_c)^2},\ \frac{\partial f}{\partial \sigma_t}=0$$

and in other regions:

$$\frac{\partial f_{n+1}^{(k)}}{\partial \sigma_c}=\frac{1}{6}(I_1-\sigma_t),\ \frac{\partial f_{n+1}^{(k)}}{\partial \sigma_{bc}}=0.0,\ \frac{\partial f_{n+1}^{(k)}}{\partial \sigma_t}=\frac{1}{6}(I_1+\sigma_c)$$

Second derivatives of the Chen-Chen loading surface are

$$\frac{\partial^2 f}{\partial \sigma^2}=n\begin{Bmatrix} 1 & 1 & 1 & 0 & 0 & 0 \\ 1 & 1 & 1 & 0 & 0 & 0 \\ 1 & 1 & 1 & 0 & 0 & 0 \\ 0 & 0 & 0 & 2 & 0 & 0 \\ 0 & 0 & 0 & 0 & 2 & 0 \\ 0 & 0 & 0 & 0 & 0 & 2 \end{Bmatrix}+\begin{Bmatrix} 2/3 & -1/3 & -1/3 & 0 & 0 & 0 \\ -1/3 & 2/3 & -1/3 & 0 & 0 & 0 \\ -1/3 & -1/3 & 2/3 & 0 & 0 & 0 \\ 0 & 0 & 0 & 2 & 0 & 0 \\ 0 & 0 & 0 & 0 & 2 & 0 \\ 0 & 0 & 0 & 0 & 0 & 2 \end{Bmatrix}$$

In the compression-compression region:

$$\frac{\partial^2 f}{\partial \sigma_{ij}\partial \sigma_c}=\frac{\sigma_c^2-4\sigma_c\sigma_{bc}+\sigma_{bc}^2}{3.0(2\sigma_{bc}-\sigma_c)^2}\delta_{ij},\ \frac{\partial^2 f}{\partial \sigma_{ij}\partial \sigma_{bc}}=\frac{2(\sigma_c^2-\sigma_c\sigma_{bc}+\sigma_{bc}^2)}{3.0(2\sigma_{bc}-\sigma_c)^2}\delta_{ij},\ \frac{\partial^2 f}{\partial \sigma_{ij}\partial \sigma_t}=0$$

and in other regions:

$$\frac{\partial^2 f}{\partial \sigma_{ij}\partial \sigma_c}=\frac{\partial^2 f}{\partial \sigma_{ij}\partial \sigma_t}=\frac{1}{6}\delta_{ij},\ \frac{\partial^2 f}{\partial \sigma_{ij}\partial \sigma_{bc}}=0$$